Dynamics of an Enzymatic Substitution Reaction in Haloalkane Dehalogenase

ARTICLE *in* JOURNAL OF THE AMERICAN CHEMICAL SOCIETY · MARCH 2004

Impact Factor: 12.11 · DOI: 10.1021/ja039093l · Source: PubMed

5 AUTHORS, INCLUDING:

Kwangho Nam
Umeå University
30 PUBLICATIONS **960** CITATIONS
SEE PROFILE

Xavier Prat-Resina
University of Minnesota Rochester
16 PUBLICATIONS **507** CITATIONS
SEE PROFILE

Mireia Garcia-Viloca
Autonomous University of Barcelona
51 PUBLICATIONS **2,336** CITATIONS
SEE PROFILE

J|A|C|S
ARTICLES
Published on Web 01/17/2004

Dynamics of an Enzymatic Substitution Reaction in Haloalkane Dehalogenase

Kwangho Nam, Xavier Prat-Resina, Mireia Garcia-Viloca, Lakshmi S. Devi-Kesavan, and Jiali Gao*

Contribution from the Department of Chemistry and Supercomputing Institute, Digital Technology Center, University of Minnesota, Minneapolis, Minnesota 55455

Received October 16, 2003; E-mail: gao@chem.umn.edu

Abstract: Reactive flux molecular dynamics simulations have been carried out using a combined QM/MM potential to study the dynamics of the nucleophilic substitution reaction of dichloroethane by a carboxylate group in haloalkane dehalogenase and in water. We found that protein dynamics accelerates the reaction rate by a factor of 2 over the uncatalyzed reaction. Compared to the thermodynamic effect in barrier reduction, protein dynamic contribution is relatively small. However, analyses of the friction kernel reveal that the origins of the reaction dynamics in water and in the enzyme are different. In aqueous solution, there is significant electrostatic solvation effect, which is reflected by the slow reorganization relaxation of the solvent. On the other hand, there is no strong electrostatic coupling in the enzyme and the major effect on reaction coordinate motion is intramolecular energy relaxation.

Introduction

The origin of the rate acceleration achieved by enzymes is one of the fundamental questions in molecular biology.[1] While experimental studies, including X-ray structural determination and site-directed mutagensis, are essential to understanding the mechanism of enzyme reactions, computer simulations can help dissect factors that are not directly amenable by experimental measurements and can provide insights into the specific interactions in the active site.[2−4] A widely used theoretical approach for studying enzyme catalysis is variational transition state theory (TST),[5−7] which gives an upper bound to the true classical rate constant

$$k = \gamma k^{\mathrm{TST}} \tag{1}$$

where k is the rate constant of a reaction, k^{TST} is the TST approximation to the rate constant, and γ is the generalized transmission coefficient.[2] In classical dynamics, the TST rate constant is the rate of one-way flux through the transition state dividing surface, which can be written as

$$k^{\mathrm{TST}} = \frac{k_{\mathrm{B}}T}{h} e^{-\Delta G^{\ddagger}/k_{\mathrm{B}}T} \tag{2}$$

where T is temperature, k_{B} is Boltzmann's constant, h is Planck's constant, and $\Delta G^{\ddagger}$ is the molar standard state quasithermodynamic free energy of activation related to the potential of mean force by $\Delta G^{\neq} = w(q^{\neq}) - w(q_{\mathrm{R}})$ with $q^{\neq}$ and q_{R} corresponding to the reaction coordinate at the transition state and reactant state, respectively. The generalized transmission coefficient at temperature T contains three components

$$\gamma(T) = \kappa(T)\Gamma(T)g(T) \tag{3}$$

which account for nonequilibrium effects, $g(T)$, tunneling, $\Gamma(T)$, and trajectories that recross the transition state separating the reactants and products, $\kappa(T)$.[2]

According to eq 1, the rate enhancement in enzyme catalyzed reactions can be achieved by lowering the free energy of activation and/or by increasing the transmission coefficient in comparison with an equivalent uncatalyzed reaction.[2,8] Equation 1 also provides a way of separating dynamic and thermodynamic factors contributing to rate enhancement, although this separation is certainly not unique because both the calculation of the potential of mean force and the transmission coefficient depend on the definition of the reaction coordinate, and involve protein fluctuations.[2,3,9,10] Experimental and computational studies show that the dominant factor responsible for the rate acceleration is the reduction of the activation barrier in the enzyme,[2,4,8,11] which is an equilibrium thermodynamic effect and can be attained both by transition state stabilization and by reactant state destabilization through interactions with specific residues in the enzyme.[2,8] The role of dynamics on enzyme catalysis, which is mainly due

(1) Wolfenden, R.; Snider, M. J. *Acc. Chem. Res.* **2001**, *34*, 938−945.
(2) Garcia-Viloca, M.; Gao, J.; Karplus, M.; Truhlar, D. G. *Science* **2004**, *303*, 186−195.
(3) Benkovic, S. J.; Hammes-Schiffer, S. *Science* **2003**, *301*, 1196−1202.
(4) Fersht, A. *Structure and Mechanism in Protein Science*; W. H. Freeman and Company: New York, 1998.
(5) Glasstone, S.; Laidler, K. J.; Eyring, H. *The Theory of Rate Processes*; McGraw-Hill: New York, 1941.
(6) Keck, J. C. *Adv. Chem. Phys.* **1967**, *13*, 85−121.
(7) Truhlar, D. G.; Garrett, B. C.; Klippenstein, S. J. *J. Phys. Chem.* **1996**, *100*, 12771−12800.
(8) Schowen, R. L. In *Transition States of Biochemical Processes*; Gandour, R. D., Schowen, R. L., Eds.; Plenum Press: New York, 1978; pp 77−114.
(9) Karplus, M. *J. Phys. Chem. B* **2000**, *104*, 11−27.
(10) Villa, J.; Warshel, A. *J. Phys. Chem. B* **2001**, *105*, 7887−7907.
(11) Warshel, A. *Computer Modeling of Chemical Reactions in Enzymes and Solutions*; Wiley: New York, 1991.

to the difference in the generalized transmission coefficient[2] between the catalyzed and uncatalyzed reaction, remains to be fully understood.[2,3,10,12,13] In this article, we determine the classical reflection contribution (recrossing), i.e., the $\kappa(T)$ factor,[2] to catalysis using reactive flux molecular dynamics simulations.[14−16] We use the nucleophilic substitution reaction between dichloroethane (DCE) substrate and Asp124 in a haloalkane dehalogenase (DHase)[17] to illustrate this computational approach (nonequilibrium and tunneling effects are expected to be small here), revealing differential dynamic effects for the reaction in water and in the enzyme.

Haloalkane dehalogenases catalyze the conversion of chlorinated hydrocarbons into alcohols and chloride ion through nucleophilic displacement by Asp124 in the active site. Because of its potential for bioremediation of environment contaminants, it has been extensively studied[17−23] and has been in fact used in applications for the treatment of contaminated soil.[24,25] The effect of barrier reduction by the enzyme has been investigated in a number of computational studies performed by modeling the active site with the substrate dichloroethane (DCE)[26−36] and by computing the potential of mean force for the nucleophilic substitution step.[37,38] The catalytic mechanism has been attributed to both desolvation effects[32−34,38] and transition state stabilization.[26−38] The present study extends previous investigations by examining the dynamics of DHase in catalysis.

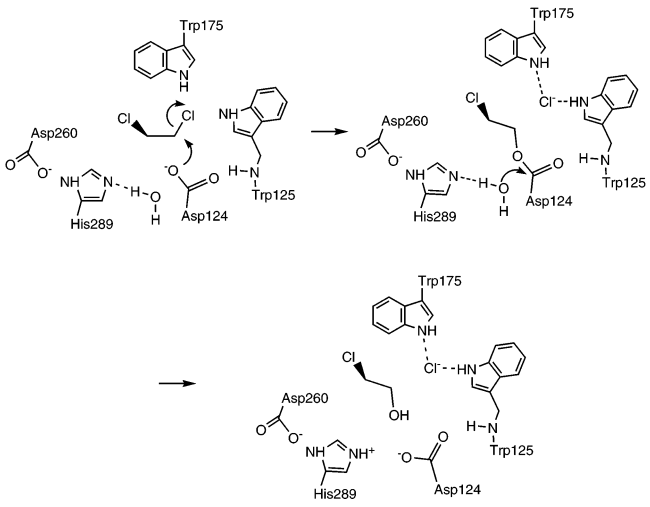

In what follows, we first describe computational details in the present study, which is followed by results and discussion. The paper concludes with a summary of major findings.

Computational Details

A. Model for the Enzyme−Substrate Complex. The X-ray crystal structure of the enzyme−substrate complex (at pH 5 and 4 °C) determined at 2.4 Å resolution (Protein Data Bank code 2DHC) was used as the starting geometry for all simulations.[17] We began with a starting configuration that was generated and fully equilibrated from a previous study using stochastic boundary molecular dynamics simulations.[38] The protonation states for all ionizable residues were set corresponding to pH 7. Thus, histidine residues were modeled as neutral residues with the proton on N_ϵ or N_δ as determined on the basis of possible hydrogen bond interactions deduced from the X-ray crystallographic structure. The resulting system has a net charge of −17 e, which was neutralized by placing sodium cations near negatively charged residues initially at distances greater than 17 Å from the active center. The final protein structure was solvated with a previously equilibrated cubic box of water molecules, centered at the geometrical mean coordinates of the protein−substrate complex. The initial dimension of the box was $65 \times 65 \times 65$ Å^3, which ensures that all protein atoms are at least 10 Å away from the edges of the box. Water molecules within 2.5 Å of any non-hydrogen atoms of the protein or existing water were removed. The final model contains 29 540 atoms, of which 4866 are protein atoms.

B. Potential Energy Surface. To equilibrate the solvated protein system, we first carried out molecular dynamic simulations under periodic boundary conditions using the all-atom CHARMM22 force field[39] to represent the protein and substrate and the three-point-charge TIP3P model for water.[40]

To model the chemical process, a combined quantum mechanical and molecular mechanical (QM/MM) potential was used in all calculations.[41−43] The enzyme−solvent system was partitioned into a quantum mechanical region consisting of 15 atoms and a molecular mechanical region containing the rest of the system. The QM system includes eight atoms from the dichloroethane (DCE) substrate and seven atoms from the side chain of Asp124. The QM subsystem contains

(12) Basner, J. E.; Schwartz, S. D. *J. Phys. Chem. B* **2004**, *108*, 444−451.
(13) Antoniou, D.; Schwartz, S. D. *J. Phys. Chem. B* **2001**, *105*, 5553−5558.
(14) Chandler, D. *J. Chem. Phys.* **1978**, *68*, 2959−2970.
(15) Montgomery, J. A., Jr.; Chandler, D.; Berne, B. J. *J. Chem. Phys.* **1979**, *70*, 4056−4066.
(16) Rosenberg, R. O.; Berne, B. J.; Chandler, D. *Chem. Phys. Lett.* **1980**, *75*, 162−168.
(17) Verschueren, K. H.; Seljee, F.; Rozeboom, H. J.; Kalk, K. H.; Dijkstra, B. W. *Nature* **1993**, *363*, 693−698.
(18) Franken, S. M.; Rozeboom, H. J.; Kalk, K. H.; Dijkstra, B. W. *EMBO J.* **1991**, *10*, 1297−1302.
(19) Pries, F.; Kingma, J.; Krooshof, G. H.; Jeronimus-Stratingh, M.; Bruins, A. P.; Janssen, D. B. *J. Biol. Chem.* **1995**, *270*, 10405−10411.
(20) Kennes, C.; Pries, F.; Krooshof, G. H.; Bokma, E.; Kingma, J.; Janssen, D. B. *Eur. J. Biochem.* **1995**, *228*, 403−407.
(21) Schanstra, J. P.; Janssen, D. B. *Biochemistry* **1996**, *35*, 5624−5632.
(22) Schanstra, J. P.; Kingman, J.; Janssen, D. B. *J. Biol. Chem.* **1996**, *271*, 14747−14753.
(23) Schindler, J. F.; Naranjo, P. A.; Honaberger, D. A.; Chang, C.; Brainard, J. R.; Vanderberg, L. A.; Unkefer, C. J. *Biochemistry* **1999**, *38*, 5772−5778.
(24) Stucki, G.; Thuer, M. *Environ. Sci. Technol.* **1995**, *29*, 2339−2345.
(25) Ridder, I. S.; Dijkstra, B. W. *CATTECH* **2000**, *3*, 126−142.
(26) Damborsky, J.; Kuty, M.; Nemec, M.; Koca, J. *J. Chem. Inf. Comput. Sci.* **1997**, *37*, 562−568.
(27) Damborsky, J.; Bohac, M.; Prokop, M.; Kuty, M.; Koca, J. *Protein Eng.* **1998**, *11*, 901−907.
(28) Dombrosky, J.; Koca, J. *Protein Eng.* **1999**, *12*, 989−998.
(29) Kuty, M.; Damborsky, J.; Prokop, M.; Koca, J. *J. Chem. Inf. Comput. Sci.* **1998**, *38*, 736−741.
(30) Lewandowicz, A.; Rudzinski, J.; Tronstad, L.; Widersten, M.; Ryberg, P.; Matsson, O.; Paneth, P. *J. Am. Chem. Soc.* **2001**, *123*, 4550−4555.
(31) Lightstone, F. C.; Zheng, Y.; Maulitz, A. H.; Bruice, T. C. *Proc. Natl. Acad. Sci. U.S.A.* **1997**, *94*, 8417−8420.
(32) Lightstone, F. C.; Zheng, Y.; Bruice, T. C. *Bio. Org. Chem.* **1998**, *26*, 169−174.
(33) Lightstone, F. C.; Zheng, Y.; Bruice, T. C. *J. Am. Chem. Soc.* **1998**, *120*, 5611−5621.
(34) Lau, E. Y.; Kahn, K.; Bash, P. A.; Bruice, T. C. *Proc. Natl. Acad. Sci. U.S.A.* **2000**, *97*, 9937−9942.
(35) Kahn, K.; Bruice, T. C. *J. Phys. Chem. B* **2003**, *107*, 6876−6885.
(36) Hur, S.; Kahn, K.; Bruice, T. C. *Proc. Natl. Acad. Sci. U.S.A.* **2003**, *100*, 2215−2219.
(37) Shurki, A.; Strajbl, M.; Villa, J.; Warshel, A. *J. Am. Chem. Soc.* **2002**, *124*, 4097−4107.
(38) Devi-Kesavan, L. S.; Gao, J. *J. Am. Chem. Soc.* **2003**, *125*, 1532−1540.
(39) MacKerell, A. D., Jr.; Bashford, D.; Bellott, M.; Dunbrack, R. L.; Evanseck, J. D.; Field, M. J.; Fischer, S.; Gao, J.; Guo, H.; Ha, S.; Joseph-McCarthy, D.; Kuchnir, L.; Kuczera, K.; Lau, F. T. K.; Mattos, C.; Michnick, S.; Ngo, T.; Nguyen, D. T.; Prodhom, B.; Reiher, W. E., III.; Roux, B.; Schlenkrich, M.; Smith, J. C.; Stote, R.; Straub, J.; Watanabe, M.; Wiorkiewicz-Kuczera, J.; Yin, D.; Karplus, M. *J. Phys. Chem. B* **1998**, *102*, 3586−3616.
(40) Jorgensen, W. L.; Chandrasekhar, J.; Madura, J. D.; Impey, R. W.; Klein, M. L. *J. Chem. Phys.* **1983**, *79*, 926−935.
(41) Field, M. J.; Bash, P., A.; Karplus, M. *J. Comput. Chem.* **1990**, *11*, 700−733.
(42) Gao, J. In *Reviews in Compututational Chemistry*; Lipkowitz, K. B., Boyd, D. B., Eds.; VCH: New York, 1995; Vol. 7, pp 119−185.
(43) Gao, J.; Truhlar, D. G. *Annu. Rev. Phys. Chem.* **2002**, *53*, 467−505.

one boundary atom: the C_α at the aspartate residue, which is represented by the generalized hybrid orbital (GHO) method.[44,45] We used the semiempirical Austin Model 1 Hamiltonian that was reparametrized by Lau et al.[34,46] to specifically treat the haloalkane dehalogenase reaction by reproducing geometrical and energetic results in comparison with high-level ab initio data in the gas phase. The AM1-SRP model of Lau et al. was optimized to fit the energies and barrier height obtained from MP2/6-31+G(d) calculations. The final AM1-SRP Hamiltonian yields an intrinsic (gas phase) barrier of 26.0 kcal/mol, which is 2.8 kcal/mol greater than the MP2 value. We note that the same model reaction between DCE and acetate has been studied at the G2 level, which gives a free energy barrier of 21.3 kcal/mol.[38] Thus, in using the AM1-SRP, one should keep in mind that it still overestimates the barrier height by 4.7 kcal/mol in comparison with ab initio G2 results. Nevertheless, such a specific reaction parametrized (SRP) model yields results with an accuracy close to the MP2 level, but it is much more computationally efficient.[34] We have adopted this AM1-SRP model in the present calculations.

C. Molecular Dynamics Simulations. To remove close contacts and highly repulsive orientations of the initial protein−solvent system, we first performed 100 steps of energy minimization for all water molecules using the adopted-basis set Newton−Raphson (ABNR) method in charmm-version c30,[47] with the protein atoms held fixed. From the resulting configuration, molecular dynamics (MD) simulations with periodic boundary conditions (PBC) and the isothermal−isobaric (NPT) ensemble at 298 K and 1 atm were carried out to obtain the average volume of the system. The constant pressure and temperature calculations were carried out using charmm-c30; in this method, a "crystal lattice" is constructed by surrounding the primary cubic cell (the ternary complex, solvent water, and the counterions) with 26 identical images. In practice, only portions of the images within a given distance are generated when a cutoff criterion is used to reduce the number of nonbonded interactions, and in all the calculations of the present study, a spherical cutoff distance of 12.0 Å was used for the nonbonded interaction generation along with a switch function in the region 10.5 to 11.5 Å to feather the interaction energy to zero. The nonbonded pair list and the image list were built on the basis of group separations, and they were updated every 25 steps and 120 steps, respectively. During an image update, the distant solvent molecules were replaced by a close image, and the group of image atoms within the cutoff distance of the primary atoms was updated.

We used the leapfrog integration scheme[48] to propagate the equations of motion with a time step of 1 fs and with the extended system constant pressure and temperature algorithm implemented in charmm.[49−51] All bond lengths and bond angles involving hydrogen atoms were constrained by the SHAKE algorithm,[52] and the dielectric constant was set to 1. Initially, the temperature of the system was gradually raised from 0 to 298 K in 30 ps of molecular dynamics. Then, a further 50 ps simulation at 298 K was carried out. The average length of the box edge in the last 1000 steps (1 ps) of the 50 ps run was 65.543 48 Å, which was used in the subsequent QM/MM molecular dynamics simulations at constant volume and temperature.

The QM/MM simulations were carried out using periodic boundary conditions and the same nonbonded cutoff, switching functions, and dielectric constant as in the MM calculations, but we used an algorithm that takes advantage of the minimum image convention for a periodic cubic box. The solvent molecules (water and counterions) were translated every 1000 steps to their image position closest to the center of the system, which is defined as the geometric center of the protein−ligand complex. The center of the protein−ligand complex was updated at each nonbonded pair list update. All the hydrogen atoms were constrained by the SHAKE algorithm. The velocity Verlet algorithm[53] and the Nosé−Hoover[49,50] constant temperature algorithm were used to run these simulations at 298 K and at constant volume on the QM-SRP/MM potential energy surface described above.

D. Potential of Mean Force Calculations. The potential of mean force (PMF) for the dehalogenation reaction of DCE by Asp124 in haloalkane dehalogenase was determined using the umbrella sampling technique[54−56] along the mass-weighted asymmetric stretch reaction coordinate q_{as}, which is defined as follows

$$q_{as} = \frac{1}{m_{Cl} + m_O}(m_{Cl}R_{CCl} - m_O R_{OC}) \tag{4}$$

where R_{OC} and R_{CCl} are the distances of the substrate C_1 carbon atom from the nucleophilic oxygen (Asp124) and the leaving group Cl^- ion, and m_O and m_{Cl} are their masses. A total of 16 separate simulations (or windows) were executed to span the entire range of the reaction coordinate from reactants to products. Each simulation was performed with the addition of a biasing potential, roughly the negative of the final computed PMF, and a harmonic restraining potential centered at the location of that particular window. For each window of these calculations, the velocities and positions of the last configuration generated in the previous window were used to initiate the next window, which was equilibrated for 15 ps, and the probability density of configurations along q_{as} was collected for an additional 50 ps and sorted into bins of width 0.0025 Å. The uncertainty in the reaction coordinate is half of the bin size, 0.00125 Å. The small bin size is due to the use of mass-weighted reaction coordinate involving a very heavy chlorine atom.

For comparison, exactly the same computational procedure was executed for the model reaction of acetate ion and dichloroethane in water. In this case, the reactants, DCE and acetate, were placed in a cubic box of about 36.8 × 36.8 × 36.8 $Å^3$, containing 1679 water molecules. The reaction coordinate was defined in the same way as the enzyme reaction in eq 4. Umbrella sampling and molecular dynamics simulations were carried out following the same procedure and lengths as in the enzyme case. There are no constraints of any kind in all simulations, both for calculations in the enzyme and in aqueous solution, and the potential of mean force was not restrained to the first solvation layer or to a small solvent cage. Typically, there is no observable ion−dipole complex for S_N2 reactions in aqueous solution,[57−60] and the results correspond to a standard state of a 1 M concentration. Additional details of these calculations can be found in ref 60.

E. Reactive Flux Trajectory Calculations. We follow the procedure of Neria and Karplus[61,62] to compute the time-dependent transmission coefficient at temperature $T = 298$ K using reactive flux calculations,[14−16] which is defined as

$$\kappa(t) = \frac{\langle \dot{q}_{as}(0) H[q_{as}(t) - q_{as}^{\neq}] \rangle_{\neq}}{1/2 \langle |\dot{q}_{as}(0)| \rangle_{\neq}} \tag{5}$$

where the brackets $\langle ... \rangle_{\neq}$ specify an equilibrium average with the reaction

(44) Gao, J.; Amara, P.; Alhambra, C.; Field, M. J. *J. Phys. Chem. A* **1998**, *102*, 4714−4721.
(45) Amara, P.; Field, M. J.; Alhambra, C.; Gao, J. *Theor. Chem. Acc.* **2000**, *104*, 336−343.
(46) Dewar, M. J. S.; Zoebisch, E. G.; Healy, E. F.; Stewart, J. J. P. *J. Am. Chem. Soc.* **1985**, *107*, 3902−3909.
(47) Brooks, B. R.; Bruccoleri, R. E.; Olafson, B. D.; States, D. J.; Swaminathan, S.; Karplus, M. *J. Comput. Chem.* **1983**, *4*, 187.
(48) Hockney, R. W. *Methods Comput. Phys.* **1970**, *9*, 136−211.
(49) Nose, S. *J. Chem. Phys.* **1984**, *81*, 511.
(50) Hoover, W. G. *Phys. Rev. A* **1985**, *31*, 1695.
(51) Anderson, H. C. *J. Chem. Phys.* **1980**, *72*, 2384.
(52) Ryckaert, J. P.; Cicotti, G.; Berendsen, H. J. C. *J. Comput. Phys.* **1977**, *23*, 327−337.
(53) Verlet, L. *Phys. Rev.* **1967**, *159*, 98.
(54) Boczko, E. M.; Brooks, C. L., III. *J. Phys. Chem.* **1993**, *97*, 4509.
(55) Kumar, S.; Bouzida, D.; Swendsen, R. H.; Kollman, P. A.; Rosenberg, J. M. *J. Comput. Chem.* **1992**, *13*, 1011.
(56) Rajamani, R.; Naidoo, K.; Gao, J. *J. Comput. Chem.* **2003**, *24*, 1775−1781.
(57) Chandrasekhar, J.; Smith, S. F.; Jorgensen, W. L. *J. Am. Chem. Soc.* **1984**, *106*, 3049−3050.

coordinate starting from the transition state, $\dot{q}_{as}(t)$ is the velocity of the reaction coordinate at time t, and $H(x)$ is a step function that equals 1 when x is positive and is 0 otherwise. The reactive flux method has been extensively used to study reaction dynamics in solution,[15,16] including S_N2 reactions,[63−67] and has recently been applied to an enzyme reaction (TIM).[61,62] We note that other approaches have also been used to determine[68] or to qualitatively examine[10,67] κ for enzyme reactions.

First, restrained molecular dynamics simulations were performed for the transition state, obtained from the potentials of mean force, both for the enzyme and aqueous system. For the enzymatic reaction, the system was first equilibrated for 15 ps, starting from a restart configuration nearest the top of the free energy barrier. Then, an additional 40 ps of calculations were carried out, and the coordinates and velocities were saved at an interval of 1 ps, resulting in a total of 40 transition state configurations. For each of the 40 transition state configurations, we propagated 100 trajectories for the reaction coordinate motion. The velocities saved from the restrained molecular dynamics simulations were used as the initial velocities to start the trajectory calculation, except one degree of freedom corresponding to the reaction coordinate, which was replaced by a velocity obtained from the Boltzmann distribution at 298 K.[61] In other studies, the initial velocities of all atoms of the transition state ensemble have been randomized in trajectory calculations.[15,16,63] Each trajectory was propagated for 100 fs, which is sufficient for computing the transmission coefficient. To test for convergency, we performed an additional set of calculations that generated 10 configurations separated by 10 ps in the restrained molecular dynamics simulation, and from these configurations, we also determined the time-dependent transmission coefficient.

The same procedure was carried out for the model reaction of an acetate ion and DCE in water. In this case, the restrained molecular dynamics simulation was run for 100 ps at the transition state, saving one structure in every 10 ps, resulting in a total of 10 transition state configurations. The transmission coefficient was computed based on 1000 to 4000 trajectories.

F. Molecular Dynamics with Constrained Reaction Coordinate. To analyze factors that contribute to the total force autocorrelation function, we computed the friction kernel at the transition state and at the reactant state (not discussed here) from additional simulations both in water and in the enzyme. Examination of the spectral density from Fourier transforms of the time-correlation functions provides insights into the difference in dynamic contributions to the enzymatic and uncatalyzed reactions. The reaction coordinate was constrained to a specified value during the molecular dynamics simulations using a SHAKE-like algorithm that we have modified using Wilson's Cartesian to internal coordinate transformation matrix.[69−71] Initially, 100 ps molecular dynamics simulations were performed for the transition state simulation. In addition, friction kernels were computed with the symmetric internal stretch fixed or with QM/MM electrostatic interactions excluded in 50 ps molecular dynamics calculations.

(58) Chandrasekhar, J.; Jorgensen, W. L. *J. Am. Chem. Soc.* **1985**, *107*, 2974−2975.
(59) Gao, J.; Xia, X. *J. Am. Chem. Soc.* **1993**, *115*, 9667−9675.
(60) Mo, Y.; Gao, J. *J. Comput. Chem.* **2000**, *21*, 1458−1469.
(61) Neria, E.; Karplus, M. *Chem. Phys. Lett.* **1997**, *267*, 26−30.
(62) Neria, E.; Karplus, M. *J. Chem. Phys.* **1996**, *105*, 10812−10818.
(63) Gertner, B. J.; Wilson, K. R.; Hynes, J. T. *J. Chem. Phys.* **1989**, *90*, 3537−3558.
(64) Gertner, B. J.; Bergsma, J. P.; Wilson, K. R.; Lee, S.; Hynes, J. T. *J. Chem. Phys.* **1987**, *86*, 1377−1386.
(65) Gertner, B. J.; Whitnell, R. M.; Wilson, K. R.; Hynes, J. T. *J. Am. Chem. Soc.* **1991**, *113*, 74−87.
(66) Whitnell, R. M.; Wilson, K. R.; Hynes, J. T. *J. Phys. Chem.* **1990**, *94*, 8625−8628.
(67) Hwang, J. K.; King, G.; Creighton, S.; Warshel, A. *J. Am. Chem. Soc.* **1988**, *110*, 5297−5311.
(68) Agarwal, P. K.; Webb, S. P.; Hammes-Schiffer, S. *J. Am. Chem. Soc.* **2000**, *122*, 4803−4812.
(69) Wilson, E. B.; Decius, J. C.; Cross, P. *Molecular Vibrations*; Dover: New York, 1980.
(70) Tobias, D. J.; Brooks, C. L., III. *J. Chem. Phys.* **1988**, *89*, 5115−5127.

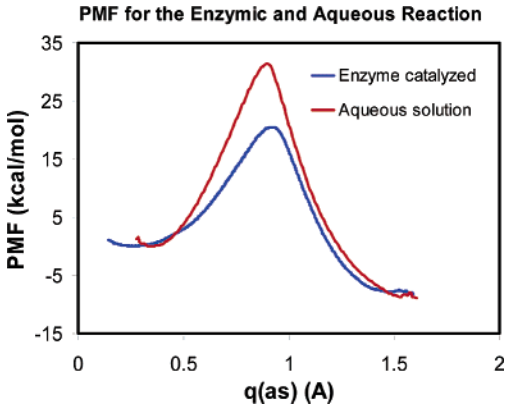

Figure 1. Computed potential of mean force for the nucleophilic substitution reaction between Asp124 and 1,2-dichloroethane in the enzyme (blue) and for the uncatalyzed reaction between an acetate ion and dichloroethane in water (red).

Results and Discussion

A. Potentials of Mean Force. The main goal of the present study is to assess dynamic contributions to catalysis using reactive flux simulations for trajectories originating from the transition state configurations. To determine the location of the transition state, potentials of mean force (PMF) as a function of q_{as} were first determined by use of umbrella sampling for the reaction both in DHase and in water (acetate ion was used in the calculation in water). The computed PMFs for the enzymatic reaction and the corresponding uncatalyzed reaction in water using the AM1-SRP Hamiltonian[34] are given in Figure 1, which provides a direct comparison of the free energy barriers of the catalyzed and uncatalyzed reaction. The transition state is located at the highest point in the PMF, which has a value of $q_{as}^{\neq} = 0.92625$ Å in DHase and 0.92300 Å in water.

In aqueous solution, the computed free energy of activation is 31.4 kcal/mol for the nucleophilic substitution reaction of DCE by an acetate ion. The enzyme DHase lowers the activation barrier to 20.5 kcal/mol. Recall that the AM1-SRP model overestimates the intrinsic (gas phase) barrier by 4.7 kcal/mol.[34] Taking this into account, we obtain a best estimate of the free energy barrier of 15.8 kcal/mol for the enzyme reaction and 26.7 kcal/mol for the uncatalyzed reaction. For comparison, the experimental free energy barrier for the dehalogenation reaction in DHase was estimated using TST to be 15.3 kcal/mol from the corresponding rate constant.[21,22,72] Early simulation results were in the range of 14[38] to 16 kcal/mol.[37] The present AM1-SRP QM/MM simulations show that the enzyme reduces the free energy activation barrier by 11 kcal/mol, smaller than the previous estimate of about 16 kcal/mol[38] but greater than that estimated by Shurki et al. (8.3 to 9.4 kcal/mol).[37]

Experimentally, the free energy of activation for the reaction of acetate ion with DCE in water has been determined to be 29.9 kcal/mol at 373 K,[73] and a free energy barrier of 28.2 kcal/mol can be obtained using $\Delta G^{\neq} = \Delta H^{\neq} - T\Delta S^{\neq}$, although it is likely that these parameters would be temperature dependent.[38] Our previous study employing the semiempirical PM3 Hamil-

(71) Lu, D. H.; Zhao, M.; Truhlar, D. G. *J. Comput. Chem.* **1991**, *12*, 376−384.
(72) Schanstra, J. P.; Ridder, I. S.; Heimeriks, G. J.; Rink, R.; Poelarends, G. J.; Kalk, K. H.; Dijkstra, B. W.; Janssen, D. B. *Biochemistry* **1996**, *35*, 13186−13195.
(73) Okamoto, K.; Kita, T.; Araki, K.; Shingu, H. *Bull. Chem. Soc. Jpn.* **1967**, *40*, 1912−1916.

tonian for the QM region with the free energy barrier corrected by ab initio G2 calculations yielded a value of 29.8 kcal/mol,[38] in good accord with the present AM1-SRP model. For comparison, Shurki et al. obtained an activation free energy of 24.9 kcal/mol using an empirical valence bond potential.[37] These authors reported an estimated experimental free energy barrier of 26 kcal/mol, although the details of their extrapolation procedure were not provided in the original paper.[37] These values are certainly too low in comparison with the experimental data from the work of Okamoto et al.[73]

Factors that contribute to the reduction of the free energy barrier have been discussed previously by analyzing solvent effects and hydrogen bonding interactions[38] and by computing electrostatic contributions.[37,38] It is well-known that solvent effects can increase the barrier heights for S_N2 reactions as much as 20 orders of magnitude.[57,74] In the present case, solvent effects increase the free energy barrier by about 6−8 kcal/mol (from the ion−dipole complex) for the reaction between DCE and acetate in water.[38] The origin of the solvent effects was well characterized by differential solvation effects between the charge-localized reactant and the charge-delocalized transition state.[57,60,75] In contrast, the active site of DHase contains only one solvent water molecule, which is the nucleophile in the subsequent deacylation step, along with two amide groups (Glu56 and Trp125) forming hydrogen bonds with the nucleophile Asp124. The major difference from the reaction in water is that, rather than being poorly solvated at the transition state due to charge delocalization, the transition state in the active site enjoys increased hydrogen bonding stabilizations from two Trp residues thanks to the development of partial negative charges on the leaving group. In ref 38, the catalytic mechanism of haloalkane dehalogenase was attributed to both desolvation effects and transition state stabilization, with about equal contribution to barrier reduction.

Bruice and co-workers used the concept of near attack conformation (NAC) to rationalize the catalytic power of DHase,[32−34] but Shurki et al. suggested that the "NAC effect" only contributes about 2 kcal/mol to barrier reduction.[37] Warshel and co-workers also carried out the most detailed analyses of electrostatic and nonelectrostatic factors for both catalyzed and uncatalyzed reactions. They found that solvent effects increase the intrinsic barrier by 10.5 kcal/mol, consistent with our results, whereas electrostatic interactions in the enzyme active site also raise the dehalogenation barrier by 4.4 kcal/mol relative to the gas-phase barrier,[37] contrary to our findings.[38] The latter result of ref 37 is surprising because the barrier in the enzyme (15.3 kcal/mol) is substantially smaller than the intrinsic barrier (21.3 kcal/mol at the G2 level of theory), and it is not clear how the barrier can be lowered in the enzyme if electrostatic interactions increase the barrier height by 4.4 kcal/mol in the active site. Nevertheless, solvation effects (or electrostatics) are reduced by 6.1 kcal/mol in the enzyme active site relative to that in solution.[37]

B. Dynamics. Although dynamic fluctuations and protein conformational changes[76−78] play an essential role in function and catalysis and can be fully characterized by the quasithermodynamic free energy of activation discussed above,[10] dynamic contribution to catalysis is concerned with the change in the generalized transmission coefficient between the catalyzed and uncatalyzed reactions.[2,3,9,10] In ref 2, three factors have been discussed, contributing to the generalized transmission coefficient (eq 3). In the present case, quantum mechanical tunneling is small because the dehalogenation reaction involves heavy atoms in the bond making and breaking processes.[38] Further, deviation from the equilibrium assumption in TST is expected to be small.[2,10] Thus, our focus is on the effect of dynamical recrossing, which is modeled by the reactive flux simulation method (eq 5).[14,16]

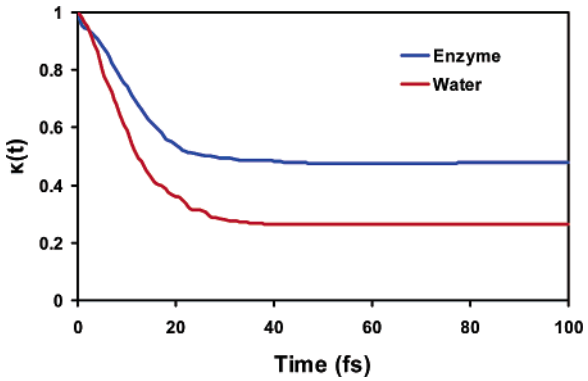

Figure 2. Computed time-dependent transmission coefficient, $\kappa(t)$, for the reaction in water (red) and in haloalkane dehalogenase (blue).

Figure 2 shows the computed time-dependent transmission coefficients for the enzymatic and aqueous reactions. The function $\kappa(t)$ equals 1 at a very short time, and it decays to a plateau, following a short period of relaxation time during which trajectories may recross the transition state until they all settle into either the reactant or product state.[14,16,61,63,65] The plateau value of $\kappa(t)$ corresponds to the transmission coefficient for the reaction. Figure 2 shows that $\kappa(t)$ reaches the plateau value within 30 fs for both the enzymatic and uncatalyzed reaction. The computed κ is 0.53 for the enzymatic process, whereas it is 0.26 for the uncatalyzed, reference reaction in water. Interestingly, the value for the enzyme reaction is similar to that (0.4) for a proton-transfer reaction in the enzyme triosephosphate isomerase.[61] Thus, in addition to the lowering of the barrier height, the enzyme further accelerates the nucleophilic substitution reaction by a factor of 2, which is substantial kinetically. However, compared to the enormous reduction of free energy barrier, which was computed to be 11−16 kcal/mol,[37,38] protein dynamic effects (about 0.5 kcal/mol in free energy term) make a rather small contribution to catalysis in DHase.

We have also tested the convergence of transition state sampling in the trajectory calculations by extending the interval of transition state configurations from 1 to 10 ps in a separate, TS-restrained molecular dynamics simulation that lasted 100 ps for the enzyme system. We repeated similar reactive flux calculations by running 100 trajectories for each of the 10 new transition-state configurations, and the computed transmission coefficient is 0.51. Thus, the effect of correlation between different initial transition state configurations is not large in the present dehalogenation reaction.

C. Differential Solvation Effects in Solution and in DHase. Further insights into the chemical dynamics are obtained by

(74) Ingold, C. K. *Structure and Mechanism in Organic Chemistry*, 2nd ed.; Cornell University: Ithaca, New York, 1969.
(75) Gao, J.; Garcia-Viloca, M.; Poulsen, T. D.; Mo, Y. *Adv. Phys. Org. Chem.* **2003**, *38*, 161−181.
(76) Gao, J. *Curr. Opin. Struct. Biol.* **2003**, *13*, 184−192.
(77) Hammes, G. G. *Biochemistry* **2002**, *41*, 8221−8228.
(78) Hammes-Schiffer, S. *Biochemistry* **2002**, *41*, 13335−13343.

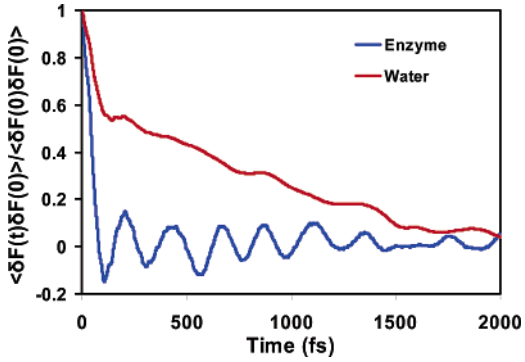

Figure 3. Autocorrelation function $<\delta F(t)\delta F(0)>$ where $\delta F(t)$ is the fluctuation in the force on the reaction coordinate at the transition state.

examining the friction kernel $\eta(t)$ of the motion of the reaction coordinate based on a non-Markovian generalized Langevin equation for the reaction in water and in the enzyme. This theoretical approach has been applied to numerous systems in the understanding of solvation effects on the dynamics of chemical processes.[63,65,79−85] The friction kernel is related to the random force, $\delta F(t)$, exerted on the reaction coordinate q_{as} by the second fluctuation dissipation theorem[80]

$$\eta(t) = \frac{1}{\mu k_B T}\langle \delta F(t)\delta F(0)\rangle \qquad (6)$$

where μ is the reduced mass of the reaction coordinate (see eq 4 for definition of the reaction coordinate). The average random force $\langle \delta F\rangle$ is zero. In addition, $\langle F\rangle = 0$, confirming that the calculation was carried out at the saddle point of the PMF. The relaxation of the time-dependent friction kernel depicts the response of solvent on the change in the reaction coordinate and reflects the dynamical coupling of the enzyme and/or solvent motions to the reaction coordinate motion. The time dependence of the friction kernel contains information on solute−solvent interactions for activated barrier crossing.[84,86] Examination of the dynamical behavior and contributing factors can provide insights into the difference in intermolecular interactions between the reactants and the environment for the reaction in the enzyme and in aqueous solution.

The key result in the present study is shown in Figure 3, which depicts the autocorrelation functions (ACF) of the fluctuation of the forces on the reaction coordinate at the transition state for the reaction in water and in the enzyme, which were determined by 100 ps constrained molecular dynamics simulations. This is sufficiently long since the barrier recrossing dynamics settles down in about 30 fs (Figure 2). Both enzymatic and aqueous reactions experience a very rapid initial relaxation process at a time scale of about 50 fs, but there are major differences in the longer time behavior. In water, the fast process is followed by a slower relaxation due to solvent reorganization, on a time scale of 1−2 ps, consistent with that

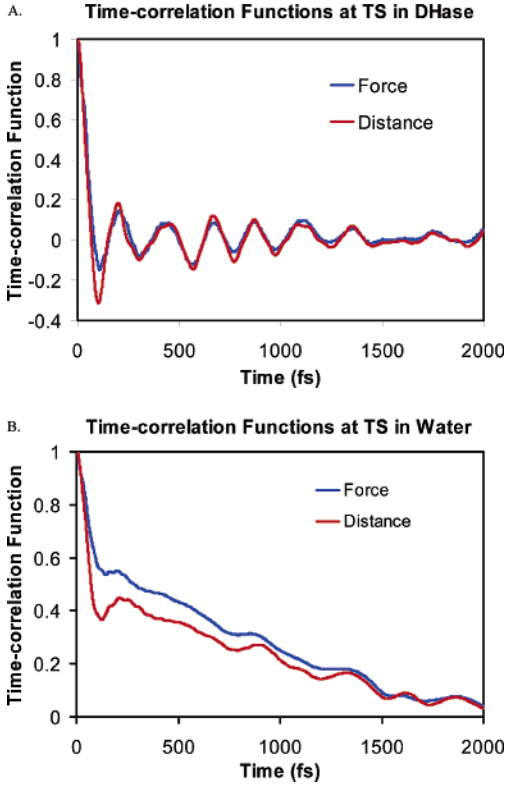

Figure 4. Computed autocorrelation functions for the fluctuating force on the reaction coordinate (blue) and the symmetric stretch distance between carbon and Asp124 nucleophilic oxygen (red) at the transition state in haloalkane dehalogenase (A) and in water (B).

of water reorientation motions in solution.[87,88] In the enzyme, the long-time relaxation process is absent, but it is replaced by a fast oscillation due to intramolecular symmetric stretch.

This assignment is confirmed by comparison with the ACF of the bond distance between the nucleophilic oxygen of the carboxylate group and the substrate carbon C_1 atom and between the C_1 and leaving Cl atom (not shown), which is the dominant component in the mass-weighted symmetric stretch coordinate. Figure 4A compares the ACFs for the total fluctuating force on the reaction coordinate constrained at the transition state and the corresponding symmetric bond fluctuation in the enzyme simulation. It can be seen that these two ACFs nearly coincide with each other, with a characteristic frequency of about 150 cm^{-1} derived from the power spectra (Figure 5). The same comparison is made for the uncatalyzed reaction in water in Figure 4B, which does not exhibit significant intramolecular contributions. The results shown in Figures 3 and 4 suggest that intermolecular hydrogen bonding interactions are dominant in aqueous solution, whereas intramolecular correlation with the reaction coordinate motion is significant in the enzyme (see below), consistent with strong desolvation effects. The different dynamic behaviors for the reaction in water and in the enzyme are also reflected by the computed friction kernel, $\eta(0)$, which is ca. 184 kcal/g Å^2 in DHase and 578 kcal/g Å^2 in water, revealing stronger interactions in water than those in the enzyme.

The different dynamic behaviors of enzymatic and aqueous reactions in Figure 3 are markedly different from that for the

(79) Grote, R. F.; Hynes, J. T. *J. Chem. Phys.* **1980**, *73*, 2715−2732.
(80) Adelman, S. A. *Adv. Chem. Phys.* **1983**, *53*, 61.
(81) Verkhivker, G.; Elber, R.; Gibson, Q. H. *J. Am. Chem. Soc.* **1992**, *114*, 7866−7878.
(82) Haynes, G. R.; Voth, G. A.; Pollak, E. *J. Chem. Phys.* **1994**, *101*, 7811−7822.
(83) Haynes, G. R.; Voth, G. A. *J. Chem. Phys.* **1995**, *103*, 10176−10182.
(84) Neria, E.; Fischer, S.; Karplus, M. *J. Chem. Phys.* **1996**, *105*, 1902−1921.
(85) Sagnella, D. E.; Straub, J. E.; Jackson, T. A.; Lim, M.; Anfinrud, P. A. *Proc. Natl. Acad. Sci. U.S.A.* **1999**, *96*, 14324−14329.
(86) Berne, B. J.; Tuckerman, M. E.; Straub, J. E.; Bug, A. L. R. *J. Chem. Phys.* **1990**, *93*, 5084−5095.
(87) Mosyak, A. A.; Prezhdo, O. V.; Rossky, P. J. *J. Chem. Phys.* **1998**, *109*, 6390−6395.
(88) Balbuena, P. B.; Johnston, K. P.; Rossky, P. J.; Hyun, J.-K. *J. Phys. Chem. B* **1998**, *102*, 3806−3814.

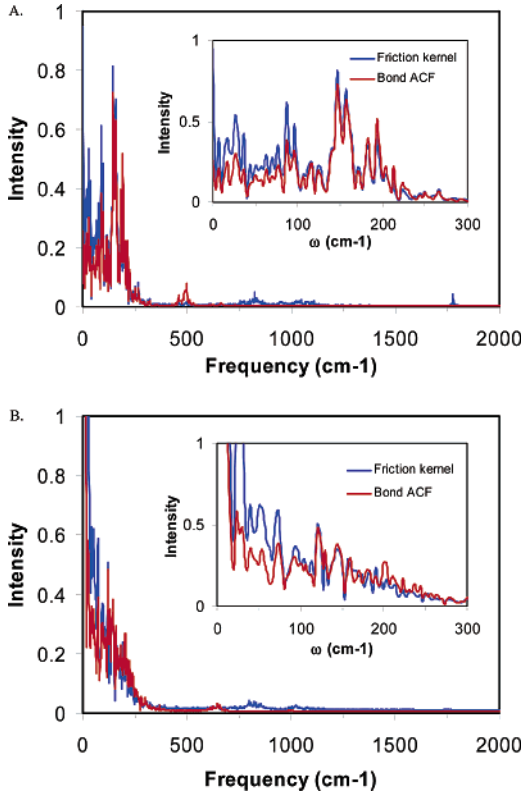

Figure 5. Power spectra of the time-correlation functions in Figure 4 for the fluctuating force on the reaction coordinate (blue) and the symmetric stretch distance between carbon and Asp124 nucleophilic oxygen (red) at the transition state in haloalkane dehalogenase (A) and in water (B).

hydride transfer reaction in liver alcohol dehydrogenase.[10] Villa and Warshel using an empirical valence bond potential found that the time-correlation functions for an energy-gap reaction coordinate, which was derived for estimating the transmission coefficient, were similar for the enzymatic and aqueous processes.[10] They concluded that there is little difference in dynamics for the enzyme catalyzed reaction and the uncatalyzed reaction in water.[89]

The analysis of the power spectra is particularly informative. By comparison with normal mode vibrational frequencies for the transition state, we can identify several key vibrational modes in the power spectra, including the symmetric stretch (150 cm^{-1}) and bending (266 cm^{-1}) involving the three atoms in bond making and breaking (note that the asymmetric stretch is the reaction coordinate), the bending (827 cm^{-1}) and asymmetric stretch (1777 cm^{-1}) of the Asp124 carboxyl group, and the bending mode (1050 cm^{-1}) of a methylene group in DCE. In addition to the direct resonant coupling of the asymmetric stretch reaction coordinate with vibrational modes of the protein bath as a route for energy transfer, the internal vibrational modes of the reactant also mediate energy transfer to the bath.[90−93] In the enzyme (Figure 5A), the power spectrum of the friction

(89) An anonymous referee points out a scenario, with which we fully agree, that the absence of a difference in transmission coefficient will not necessarily indicate that there is no dynamic effect: One can construct models in which degrees of freedom couple to the reaction coordinate and modulate barriers. When these degrees of freedom are turned on and off, there will be no indication in the transmission coefficient, but they strongly affect the rate in classical TST. See also ref 43.

(90) Bader, J. S.; Berne, B. J. *J. Chem. Phys.* **1994**, *100*, 8359−8366.
(91) Rey, R.; Hynes, J. T. *J. Chem. Phys.* **1996**, *104*, 2356−2368.
(92) Skinner, J. L.; Park, K. *J. Phys. Chem. B* **2001**, *105*, 6716−6721.
(93) Lawrence, C. P.; Skinner, J. L. *J. Chem. Phys.* **2003**, *119*, 1623−1633.

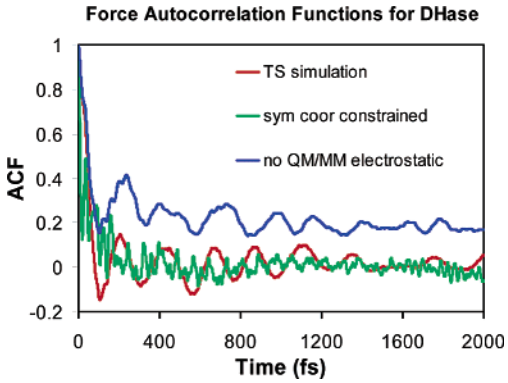

Figure 6. Computed autocorrelation function (ACF) of the force fluctuation on the reaction coordinate at the transition state (red), and ACFs computed with both the symmetric and asymmetric coordinate constrained (green) and without QM/MM electrostatic interactions (blue) for the dehalogenation reaction in the enzyme.

kernel shows significant intensities in the low-frequency region (<100 cm^{-1}) due to protein dynamic fluctuations, while considerable contributions from faster modes are also observed (e.g., the carbonyl stretch at ca. 1800 cm^{-1}). The characteristic fast oscillations in Figures 3 and 4a correspond to the internal symmetric stretch at 150 cm^{-1} with dominant intensity in the power spectra, a strong indication of weak interactions with the environment. On the other hand, the power spectrum of the friction kernel in water shows major contributions from reorientation and translation motions of the solvent water and low intensities near the carboxyl bending and stretching modes in high-frequency regions (Figure 5B). The intensity of the symmetric stretch mode is also much smaller than in the enzyme. These results demonstrate that intermolecular interactions with water dominate energy transfer from the reaction coordinate motion, suggesting a more direct coupling of water with the reaction coordinate, in contrast to the enzymatic process where intramolecular vibrations provide a main channel for coupling the enzyme environment to the reaction coordinate.

We attribute the difference in the molecular dynamics between the enzymatic and aqueous dehalogenation reaction to different electrostatic environments. Previously, we and others have found that there is a major desolvation effect in the DHase reaction, contributing 6 to 8 kcal/mol to the reduction of the activation barrier (see above).[31−36,38] Figure 3 already shows the difference of the solvent relaxation time in water and the significance of intramolecular symmetric stretch in the enzyme. In Figures 6 and 7, we further examine the individual factors that contribute to the computed ACF of the total fluctuating force on the reaction coordinate at the transition state. We carried out two additional simulations; in one case, both the symmetric and asymmetric coordinates are constrained (i.e., fixing the two distances for the breaking and forming bonds) at the transition state, and in the second, QM/MM (i.e., reactant and environment) electrostatic interactions are excluded (of course, electrostatic interactions are kept for all other parts of the system). Figure 6 compares the ACF of the total fluctuating force on the reaction coordinate (Figure 3) with the ACFs of the two additional cases, at the transition state in the enzyme. When the symmetric coordinate is also constrained, in addition to the asymmetric reaction coordinate, the characteristic symmetric oscillations in the total force fluctuation ACF (red curve) vanishes (green curve in Figure 6). The long-time relaxation

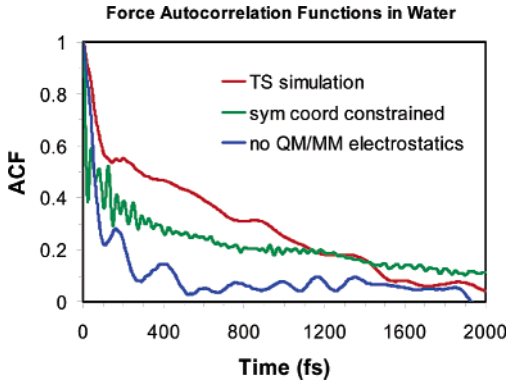

Figure 7. Computed autocorrelation function (ACF) of the force fluctuation on the reaction coordinate at the transition state (red), and ACFs computed with both the symmetric and asymmetric coordinate constrained (green) and without QM/MM electrostatic interactions (blue) for the nucleophilic substitution reaction between dichloroethane and acetate ion in water.

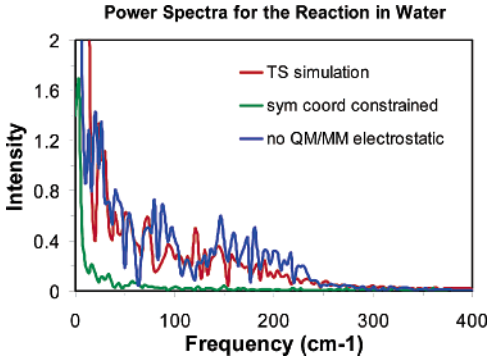

Figure 8. Fourier transform of the autocorrelation functions in Figure 7 for the dehalogenation reaction in water.

behavior due to electrostatic and van der Waals interactions in the symmetric stretch constraint is not further assessed here, but the fast dynamic fluctuations of other amino acid residues in the active site that affect the electrostatic interactions with the QM region are apparent in the green curve. However, the signature of these interactions only shows up after the dominant intramolecular motion is frozen. When electrostatic interactions between the QM and MM regions are excluded in the simulation (blue curve), the symmetric stretch motion remains, and a very long relaxation process due to van der Waals interactions is observed.

Turning to similar comparisons for the uncatalyzed reaction in water in Figure 7, we found that the solvent relaxation time in the ACF obtained with both the symmetric and asymmetric coordinates constrained (green) is about twice as long as that for the ACF of the total fluctuating force on the asymmetric coordinate (red). Clearly, the symmetric vibration helps energy transfer between the solute and solvent as well, which enhances the water reorientation process in the first solvation layer. This is reflected by the corresponding power spectra in Figure 8 (the high frequency region has very low intensity and is not shown for clarity), in which the intensity is severely reduced even in the very low-frequency region (green) in the case where both the symmetric and asymmetric coordinates are constrained. When the electrostatic interactions between the QM and MM regions are screened out (blue), we see that the intensity corresponding to the internal symmetric stretching motions increases (Figure 7). Interestingly, the impact of the solvent

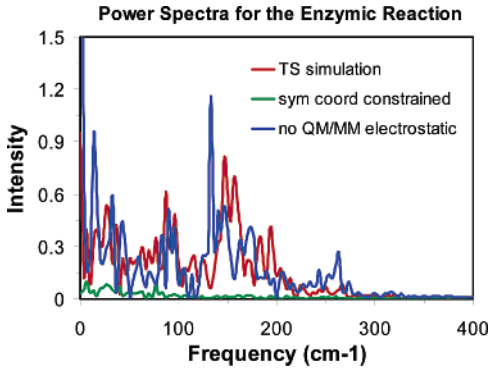

Figure 9. Fourier transform of the autocorrelation functions in Figure 6 for the dehalogenation reaction in the enzyme.

libration motions on solute−solvent coupling is not significantly affected in this case. This is because the dynamics of the environment is similar, and it is effectively coupled to the QM region through van der Waals interactions.

It is interesting to compare the power spectra obtained for the enzymatic reaction with different constraints and excluding QM/MM electrostatic interactions (Figure 9). When QM/MM electrostatic interactions are removed (blue), the symmetric stretch is red-shifted by about 15 wavenumbers. However, when both the symmetric and asymmetric coordinates are fixed at the transition state, the protein dynamical fluctuations are not reflected in the power spectra, and there is no coupling with the protein environment at the low-frequency regions as opposed to the situation in water, in which weaker coupling is still apparent under the same constraints (Figure 8). This further shows the differential environment effects on reaction coordinate motions in water and in the enzyme.

Conclusions

In conclusion, we have studied the dynamics of the nucleophilic substitution reaction of DCE by a carboxylate group in DHase and in water using combined QM/MM potential and reactive flux molecular dynamics simulation methods. We found that protein dynamics accelerates the reaction rate by a factor of 2 over the uncatalyzed reaction or lowers the free energy barrier by about 0.5 kcal/mol. However, in comparison with the large thermodynamic effect in barrier reduction (about 11 to 16 kcal/mol),[37,38] protein dynamic contribution is rather small. This conclusion is in agreement with previous findings for other enzyme systems.[2,3,10] The discovery in the present study is that the origins of the reaction dynamics for the uncatalyzed process in water and the catalyzed reaction in the enzyme are different from analyses of the friction kernel for the reaction coordinate motions. In aqueous solution, there is a significant electrostatic solvation effect, which is reflected by the slow reorganization relaxation of the solvent. On the other hand, there is no strong electrostatic coupling in the enzyme and the major effect on reaction coordinate motion is intramolecular energy relaxation.

Acknowledgment. We thank the National Institutes of Health for support of our research on enzyme catalysis. We also thank Professors Martin Karplus and Donald G. Truhlar for insightful comments on an early version of this manuscript.

JA039093L